An Analytical Solution for Large Displacements of End-Loaded Beams

Christian Iandiorio, Pietro Salvini

An Analytical Solution for Large Displacements of End-Loaded Beams

C. Iandiorio ; P. Salvini *

Dept. of Enterprise Engineering University of Rome "Tor Vergata"

* E-mail of corresponding Author: salvini@uniroma2.it

Abstract

The paper presents a closed-form analytical solution for the finite displacement analysis of cantilever beams end-loaded, having an unvarying section. Extension to supported beams loaded at the middle point is obvious. The solution accounts of slender beams, so that shear deformation effect is neglected. Material elasticity holds. Concentrated end loads are considered within the solution. Several former approaches to this classical problem can be found in the scientific literature. Typical methods provides an integral form, solved by means of incomplete elliptic functions. Alternatively, a massive number of numerical integrations techniques have been proposed, such as "Non linear shooting method", "Automatic Taylor expansion technique (ATET)", "Runge-Kutta method", etc...

In the present paper, the solution is gained through a parametric representation of the average line of the bending beam, after an expansion based on Gaussian hypergeometric functions. One of the main advantage is that an end-to-end analysis is possible, thus avoiding the integration throughout the full length of the beam. The method considers straight lines as well as circular shaped lines; the way to shift between the two cases is suggested within the paper. The reference system to get an easier solution of the integrals is taken so that it is aligned with the resulting load applied. Graphic presentations of some examples compare the analytic solutions here provided with numerical solutions, finite element method results and an experimental evidence.

Keywords: Large Displacements Beams, Hypergeometric Series, Analytic solution.

1 Introduction

As well known, beams have several applications in mechanical and civil engineering. In most cases, the structures are subjected to systems of forces causing small displacements. However, there are applications of practical interest in which this condition is not satisfied and the structures experience large displacements, while remaining within the elastic response of the material. This occurs e.g. for many classes of slender beams, springs, wires and so on.

Notable examples are the design of arrow bows, helicopter rotor blades [1], airplane wings, MEMS (Micro-ElectroMechanical Systems) technology.

Non-linear behavior of beams may rise essentially for two reasons: material response and geometric non-linearity. Geometrical nonlinearity arises from equilibrium equations, which decline differently if the undeformed or deformed shape is considered.

The first formulation to this problem dates back to 1691 by James Bernoulli who provided a first solution. Euler worked on it half a century later (1742) and in 1744 published the book "*Methodus inveniendi lineas curvas maximi minimive proprietate gaudentes, sive solutio problematis isoperimetrici lattissimo sensu accepti*" where in the appendix he reported the complete solution of the problem called by him "Elastica" [2]. A sort of variational methods where first used to get the solution. From a Mathematical point of view the problem seemed solved, but, in the Euler formulation it was difficult to figure out any technical application. In 1944 [3] and 1945 [4] this problem was reformulated in the case of a cantilever beam, with constant section and subjected to a vertical load. They made use of intrinsic geometry, which allows a parametric description of the flexible beam; an almost analytical solution was reached through incomplete elliptical integrals.
As it is known, a solution employing elliptic integrals involves the use of numerical integration, even if this is masked when referring to look-up tables. Other authors solved the differential equations by means of various numerical integration techniques, such as "Non linear shooting method" [5], "Automatic Taylor expansion technique (ATET)" [6], "Numerov's method" [7], "Runge-Kutta method" [8], etc.
The goal of this paper is to present an analytical solution for finite displaced beams, in the elastic material response, using the Gaussian hypergeometric series. This allows a quadrature of the trigonometric integrals, which are recurrent in the present paper, looking for the solution by a parametric approach. The interest of an analytical solution is due to the fact that solving a non-linear problem numerically (i.e. non-linear ODE) it is not a trivial operation. Even the simpler problems require advanced numerical methods and refined discretization to avoid instability of the solution. Moreover, the advantage of having an analytical solution is that one can identify in a clearer form the effect of the parameters that govern the solution, seeking for an optimal parameter choice. The present paper provides a solution in closed form for cantilever beams with loads concentrated at the end, easily extended to supported beams loaded in the middle. Beams can have an initial curvature in the undeformed configuration through the addition of a parameter. Since consistent displacements of mono dimensional elements in the elastic domain are possible only for slender beams, it is straightforward to discard shear deformation and to consider a linear strain slope over the section.

2 Mathematical model formulation

The mathematical model here discussed, capable to obtain a solution in closed form of a beam subjected to large displacements, requires the following fundamental assumptions:

- Small strain hypothesis;
- The material constituting the beam is linear elastic, homogeneous and isotropic;
- The shear effect is neglected (Euler-Bernoulli-Navier beam theory);
- Constant section of beam.

Kinematics compatibility equations:
When large displacements occurs, the angle of rotation cannot be mixed up with its tangent. Referring to Fig. 1, being s the curvilinear abscissa, ψ_0 the angle giving the initial tangent direction at any point by respect to the x-axis, ψ the final angle of rotation, the change in slope is given by:

$$\varphi(s) = \psi(s) - \psi_{in}(s) \tag{1}$$

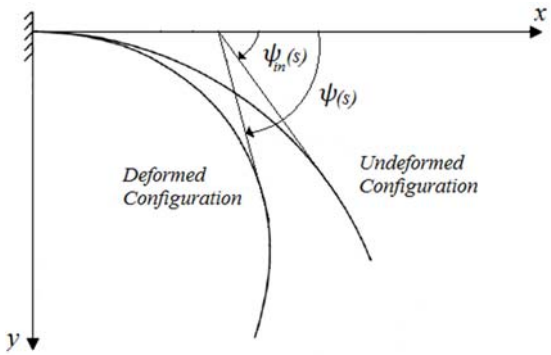

Fig. 1. A schematic view of how in large displacements, the angle of the unit tangent vector cannot be considered small

Moment-curvature relationship:
Known that in the Euler-Bernoulli-Navier beam theory $M(s)/EI = d\varphi(s)/ds$ (here M is considered positive clockwise), where EI is the flexural stiffness (considered constant along the beam). By deriving the equation (1) with respect to the arc length:

$$k(s) - k_{in}(s) = \frac{M(s)}{EI} \tag{2}$$

Where $k = \frac{d\psi}{ds}$ is the curvature of the middle beam line in the deformed configuration at the curvilinear abscissa s, and $k_{in} = d\psi_{in}/ds$ is the curvature of the middle beam line in the initial configuration. The sign of the curvature corresponds to the sign of the y position of the center of curvature.

Static equilibrium:
The equations take advantage of the geometric representation given in Fig. 2. Isolating a section of the curve between points P_1 and P_2 ; $\|\overline{P_1P_2}\| = ds$ and being: $\boldsymbol{N}$ the normal force (tension), $\boldsymbol{T}$ the shear force, $\boldsymbol{M}$ the bending moment and $\boldsymbol{q}$ the distributed load vector, the static equilibrium to translation on x and y directions and to rotation around z take the form:

$$\begin{cases} \dfrac{d}{ds}[N\cos(\psi) - T\sin(\psi)] + q_x = 0 \\ \dfrac{d}{ds}[N\sin(\psi) + T\cos(\psi)] - q_y = 0 \\ \dfrac{dM}{ds} + T = 0 \end{cases} \tag{3}$$

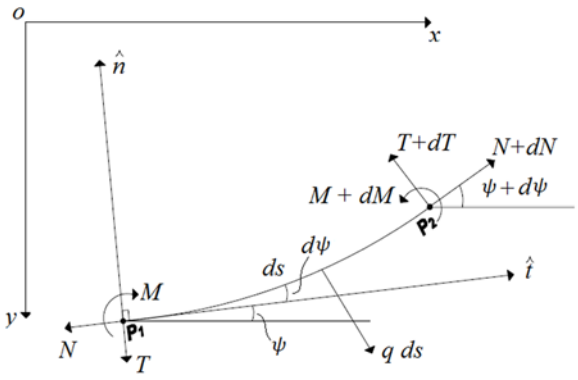

Fig. 2. Infinitesimal curve section

Integrating the first two equations of (3) from zero to the generic curvilinear abscissa *s*, multiplying the first by *sin(ψ)* and the second by *cos(ψ)*, adding them and substituting to the third one gives a new bending equilibrium equation emerges:

$$\begin{aligned} &\frac{\mathrm{dM}}{\mathrm{ds}} + \left[(T\sin\psi)\Big|_{s=0} - (N\cos\psi)\Big|_{s=0} + q_x s\right]\sin(\psi) + \\ &+ \left[(T\ \cos\psi)\Big|_{s=0} + (N\sin\psi)\Big|_{s=0} + q_y s\right]\cos(\psi) = 0 \end{aligned} \tag{4}$$

Using eq. (2) and (4) one obtain the generic differential equation of static equilibrium, which in the case of a cantilever beam $\psi\Big|_{s=0} = \psi_0 = 0$ subject to a system of concentrated loads $\{F_x, F_y, M\}$ applied to the free end and distributed loads $\{q_x\ , q_y\}$ is:

$$EI\left(\frac{d^2\psi}{ds^2} - \frac{d^2\psi_{in}}{ds^2}\right) + [\pm F_x \pm q_x s\ ]sin(\psi) + \left[\pm F_y \pm q_y\ s\ \right]cos(\psi) = 0 \tag{5}$$

Where F_x, q_x are considered positive if directed opposite to the *x* axis, and F_y, q_y are considered positive if directed as the *y* axis (see Fig.1 for the reference of Cartesian axis). The application of the differential equation (5) to the whole curve allows to integrate the components of the tangent unit vector so having the new parametric geometry:

$$x(s) = x(0) + \int_0^s cos(\psi)\, ds$$

$$y(s) = y(0) + \int_0^s sin(\psi)\, ds$$

The integration of eq. (5) requires the knowledge of boundary values for ψ and ψ' in specific points. For the cantilever beam the first boundary is known at the clamping, the second one is straightforward at the free end. In the next section the parameter defining the Cartesian displacements is moved to ψ, but this change requires to be accomplished an additional (or closing) statement that is the isoperimetric condition (length preservation). This last is available since longitudinal extension is neglected when compared to bending displacements. For a model that also takes into account longitudinal section strain see [9]).

3 Analytical solutions

In this paragraph the two cases of bended- compressed or bended- tensioned beams are discussed separately. In fact the two configurations present complementary techniques in the integration of the equations on the two orthogonal directions.
Fig. 3 shows the static scheme of a cantilever beam with constant initial curvature subjected to a system of concentrated forces and torque $\{F_x, F_{y,} M\}$. Two forces F_x are reported; the one with the continuous line is associated to the bended and compressed configuration, the one with the dotted line is associated to the bended and tensioned configuration.

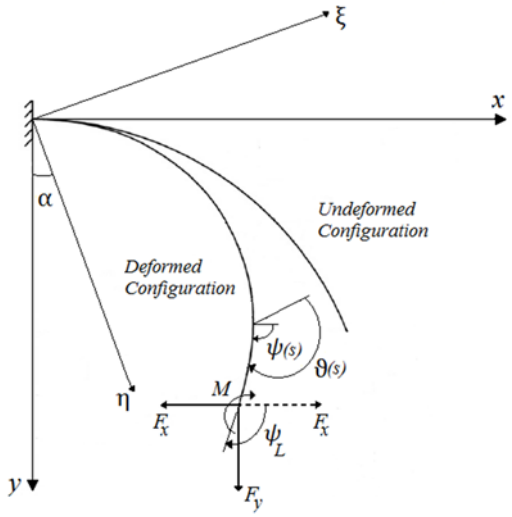

Fig. 3. Cantilever beam, bended and tensioned (dot) or bended and compressed (continuous)

3.1 Initial constant curvature cantilever beam bended and compressed

Let us consider a beam with constant initial curvature k_{in}, length L, subjected to a concentrated torque M, a force F_y directly in line with the y axis and a force F_x opposite directed to the x axis (continuous line in Fig.3), applied at the free end. The reference system adopted provides the x axis being positioned and oriented as the constrained end. In this configuration, the differential equation (5) is:

$$EI\frac{d^2\psi}{ds^2} + F_x sin(\psi) + F_y cos(\psi) = 0$$

With simple substitution steps the same becomes:

$$\frac{d^2\psi}{ds^2} + A\sin(\psi + \alpha) = 0 \tag{6}$$

Where: $A = \frac{\sqrt{{F_x}^2 + {F_y}^2}}{EI}$; $tg(\alpha) = \frac{F_y}{F_x}$

By turning the reference $\{x, y\}$ of an α angle counterclockwise, you get a new reference $\{\xi, \eta\}$, respecting the following cardinal equations in intrinsic geometry:

$$\begin{cases} \vartheta(s) = \psi(s) + \alpha \\ \frac{d\xi}{ds} = cos(\vartheta) \\ \frac{d\eta}{ds} = sin(\vartheta) \end{cases} \tag{7}$$

In this new reference, equation (6) becomes:

$$\frac{d^2\vartheta}{ds^2} + A\sin(\vartheta) = 0 \tag{8}$$

Using the substitution $\frac{d\vartheta}{ds} = Z(\vartheta)$ eq. (8) converts into:

$$Z\frac{dZ}{d\vartheta} + A\,sin(\vartheta) = 0$$

The integration of the above equation takes advantage of the variable separation:

$$\frac{(\vartheta')^2}{2} - A\,cos(\vartheta) + c_1 = 0 \qquad \left(\vartheta' = \frac{d\vartheta}{ds}\right)$$

The full solution also requires some boundary conditions.
From eq. (2) $\psi'_L = \vartheta'_L = k_{in} + \frac{M}{EI}$

$$\vartheta' = \sqrt{2A(cos\vartheta - cos\vartheta_L) + \left(k_{in} + \frac{M}{EI}\right)^2}$$

Whence one observe that $\vartheta_L = \psi_L + \alpha$:

$$ds = \frac{d\vartheta}{\sqrt{2A[cos(\vartheta) - cos(\psi_L + \alpha)] + \left(k_{in} + \frac{M}{EI}\right)^2}} \tag{9}$$

Using this last equation together with eq.s (7) we obtain the parametric equations of the final configuration of the beam, in the reference$\{\ \xi,\ \eta\ \}$; remember that $\xi_0 = 0$, $\eta_0 = 0$:

$$\eta(\psi) = \int_{\alpha}^{\psi+\alpha} \frac{\sin(\vartheta)}{\sqrt{2A[cos(\vartheta) - cos(\psi_L + \alpha)] + \left(k_{in} + \frac{M}{EI}\right)^2}}\, d\vartheta \tag{10}$$

It's easy to observe that we fall into an Abelian's integral; after extremal substitution it gives:

$$\eta(\psi) = \frac{2}{\sqrt{2A}}\left\{\sqrt{\cos(\alpha) - \left[cos(\psi_L + \alpha) - \frac{\left(k_{in} + \frac{M}{EI}\right)^2}{2A}\right]} + \right.$$

$$\left. - \sqrt{\cos(\psi + \alpha) - \left[cos(\psi_L + \alpha) - \frac{\left(k_{in} + \frac{M}{EI}\right)^2}{2A}\right]}\right\}$$

Whereas for the abscissa one obtain:

$$\xi(\psi) = \int_{\alpha}^{\psi+\alpha} \frac{\cos(\vartheta)}{\sqrt{2A[cos(\vartheta) - cos(\psi_L + \alpha)] + \left(k_{in} + \frac{M}{EI}\right)^2}}\, d\vartheta = \tag{11}$$

$$= \frac{1}{\sqrt{2A}} \int_{\alpha}^{\psi+\alpha} \left\{ \frac{d\sin(\vartheta)}{\sqrt{\cos(\vartheta) - \left[cos(\psi_L + \alpha) - \frac{\left(k_{in} + \frac{M}{EI}\right)^2}{2A} \right]}} \right\}$$

This trigonometric integral is much less trivial than the previous one. It does not allow primitive through the use of standard rules. As mentioned in the introduction, in literature the solution of this type of integral has been squared using a couple of changes of variables. This allow to obtain an analytical solution in the form of sums and differences of incomplete elliptic integrals of first and second species.
Here we propose a different approach, which uses the generalization to real coefficients of the binomial expansion and the Gaussian hypergeometric series.
It is important to highlight that incomplete elliptic integrals are usually estimated by the use of Lauricella's series [10], which contains 3 concatenated series, while by means of the adopted approach the solution is obtained as a series of hypergeometric functions (hence double infinite series non-concatenated), thus providing a computational advantage. As one can see, the solution makes use of the Euler Gamma function $\Gamma(\cdot)$ and the Gauss Hypergeometric Series ${}_2F_1(\cdot,\cdot;\cdot;\cdot)$.
For developments, see the paragraph 6.3 of the mathematical appendix.

$$\xi(\psi) = \frac{1}{\sqrt{2A}} \sum_{n=0}^{\infty} \frac{\Gamma\left(\frac{1}{2}+n\right)}{\Gamma\left(\frac{1}{2}\right) n!} \left[cos(\psi_L + \alpha) - \frac{\left(k_{in} + \frac{M}{EI}\right)^2}{2A} \right]^n \cdot$$

$$\left[{}_2F_1\left(\frac{1}{2}, \frac{2n+1}{4}; \frac{3}{2}; sin^2(\psi+\alpha)\right) sin(\psi+\alpha) - {}_2F_1\left(\frac{1}{2}, \frac{2n+1}{4}; \frac{3}{2}; sin^2(\alpha)\right) sin(\alpha) \right]$$

The parametric equations of the final configuration of the beam, with respect to the reference $\{x, y\}$, are therefore:

$$\begin{cases} x(\psi) = \xi(\psi)cos(\alpha) - \eta(\psi)sin(\alpha) \\ y(\psi) = -\xi(\psi)sin(\alpha) + \eta(\psi)cos(\alpha) \end{cases} \qquad \psi \in [0, \psi_L] \qquad (12)$$

Imposing the isoperimetric condition (length conservation) at the integral of eq. (9) it's possible to obtain the final value of the angle ψ_L:

$$L = \int_{\alpha}^{\psi_L+\alpha} \frac{d\vartheta}{\sqrt{2A[cos(\vartheta) - cos(\psi_L + \alpha)] + \left(k_{in} + \frac{M}{EI}\right)^2}} =$$

$$= \frac{1}{\sqrt{2A}} \int_{\alpha}^{\psi_L+\alpha} \frac{d\vartheta}{\sqrt{cos(\vartheta) - \left[cos(\psi_L + \alpha) - \frac{\left(k_{in} + \frac{M}{EI}\right)^2}{2A}\right]}} \qquad (13)$$

This integral can be solved again through hypergeometric Series and its development is given in Appendix 6.4.

$$L = \frac{1}{\sqrt{2A}} \sum_{n=0}^{\infty} \frac{\Gamma\left(\frac{1}{2}+n\right)}{\Gamma\left(\frac{1}{2}\right) n!} \left[cos(\psi_L + \alpha) - \frac{\left(k_{in} + \frac{M}{EI}\right)^2}{2A}\right]^n \cdot$$

$$\left[{}_2F_1\left(\frac{1}{2}, \frac{2n+3}{4}; \frac{3}{2}; \sin^2(\psi_L + \alpha)\right) \sin(\psi_L + \alpha) - {}_2F_1\left(\frac{1}{2}, \frac{2n+3}{4}; \frac{3}{2}; \sin^2(\alpha)\right) \sin(\alpha)\right]$$

Observation:
When $F_x = 0$ the solution turns impossible, this case is embedded in the next paragraph, where the direction of the axial load is inverted.

3.2 Initial constant curvature cantilever beam bended and <u>tensioned</u>

Consider a beam with constant initial curvature k_{in} , of length *L*, subjected to a concentrated torque *M*, to a force $\{F_x , F_y\}$ being now both oriented as the Cartesian axes (in this configuration the force F_x is indicated by a dotted line in Fig.3). In this configuration the differential equation (5) becomes:

$$EI\frac{d^2\psi}{ds^2} - F_x sin(\psi) + F_y cos(\psi) = 0$$

Whence:

$$\frac{d^2\psi}{ds^2} + A\cos(\psi + \alpha) = 0$$

Where $A = \frac{\sqrt{{F_x}^2 + {F_y}^2}}{EI}$; $tg(\alpha) = \frac{F_x}{F_y}$

Through the same developments and reasoning seen in 3.1, one obtain:

$$ds = \frac{d\vartheta}{\sqrt{2A[sin(\psi_L + \alpha) - sin(\vartheta)] + \left(k_{in} + \frac{M}{EI}\right)^2}}$$

From which, as seen above, the parametric equations of the curve are obtained in the {ξ , η} reference:

$$\xi(\psi) = \int_{\alpha}^{\psi+\alpha} \frac{cos(\vartheta)}{\sqrt{2A[sin(\psi_L + \alpha) - sin(\vartheta)] + \left(k_{in} + \frac{M}{EI}\right)^2}}\, d\vartheta$$

Similarly to (10) this is also an Abelian's integral; solving it:

$$\xi(\psi) = \frac{2}{\sqrt{2A}} \left\{ \sqrt{\left[sin(\psi_L + \alpha) + \frac{\left(k_{in} + \frac{M}{EI}\right)^2}{2A} \right] - \sin(\alpha)} + \right.$$

$$\left. - \sqrt{\left[sin(\psi_L + \alpha) + \frac{\left(k_{in} + \frac{M}{EI}\right)^2}{2A} \right] - \sin(\psi + \alpha)} \right\}$$

The other coordinate now requires the occurrence of the Gauss Hypergeometric functions:

$$\eta(\psi) = \int_{\alpha}^{\psi+\alpha} \frac{sin(\vartheta)}{\sqrt{2A[sin(\psi_L + \alpha) - sin(\vartheta)] + \left(k_{in} + \frac{M}{EI}\right)^2}} d\vartheta = \qquad (14)$$

$$= -\frac{1}{\sqrt{2A}} \int_{\alpha}^{\psi+\alpha} \left\{ \frac{d\cos(\vartheta)}{\sqrt{\left[sin(\psi_L + \alpha) + \frac{\left(k_{in} + \frac{M}{EI}\right)^2}{2A} \right] - \sin(\vartheta)}} \right\}$$

As can be seen, this integral results to be similar but different to (11). Using the same mathematical tools mentioned to square the integral (11), a new set of hypergeometric functions holds, different from those previously obtained. For developments, refer to paragraph 6.5 of the mathematical appendix.

$$\eta(\psi) = \frac{1}{\sqrt{2A}} \sum_{n=0}^{\infty} \frac{\Gamma\left(\frac{1}{2}+n\right)}{\Gamma\left(\frac{1}{2}\right) n!} \left[sin(\psi_L + \alpha) + \frac{\left(k_{in} + \frac{M}{EI}\right)^2}{2A} \right]^{-\left(\frac{1}{2}+n\right)} \cdot$$

$$\left[{}_2F_1\left(\frac{1}{2}, -\frac{n}{2}; \frac{3}{2}; cos^2(\alpha)\right) \cos(\alpha) - {}_2F_1\left(\frac{1}{2}, -\frac{n}{2}; \frac{3}{2}; cos^2(\psi + \alpha)\right) cos(\psi + \alpha) \right]$$

The parametric equations of the curve in the Cartesian reference $\{x, y\}$ is again (12).

The closing equation that allows to obtain the angle ψ_L is slightly different:

$$L = \int_{\alpha}^{\psi_{L+\alpha}} \frac{d\vartheta}{\sqrt{2A[sin(\psi_L + \alpha) - sin(\vartheta)] + \left(k_{in} + \frac{M}{EI}\right)^2}} =$$

$$= \frac{1}{\sqrt{2A}} \int_{\alpha}^{\psi_L+\alpha} \frac{d\vartheta}{\sqrt{\left[sin(\psi_L + \alpha) + \frac{\left(k_{in} + \frac{M}{EI}\right)^2}{2A} \right] - sin(\vartheta)}} \tag{15}$$

This integral can be solved again through hypergeometric Series and its development is given in Appendix 6.6.

$$L = \frac{1}{\sqrt{2A}} \sum_{n=0}^{\infty} \frac{\Gamma\left(\frac{1}{2}+n\right)}{\Gamma\left(\frac{1}{2}\right) n!} \left[sin(\psi_L + \alpha) + \frac{\left(k_{in} + \frac{M}{EI}\right)^2}{2A} \right]^{-\frac{1}{2}-n} \cdot$$

$$\left[{}_2F_1\left(\frac{1}{2}, \frac{1-n}{4}; \frac{3}{2}; \cos^2(\alpha)\right) \cos(\alpha) - {}_2F_1\left(\frac{1}{2}, \frac{1-n}{4}; \frac{3}{2}; \cos^2(\psi_L + \alpha)\right) \cos(\psi_L + \alpha) \right]$$

4 Numerical applications and experimental evidence

This section shows examples of the application of the outcomes obtained in the previous sections. The analytic solution here proposed was compared, for each example, with a numerical solution obtained by Gauss integration method and a solution based on the finite element method (FEM). In particular, the following paragraph offers also a comparison with the displacements obtained by an experimental test.

4.1 Straight cantilever beam subject to a vertical load

Consider the simple case of a straight cantilever beam subjected to a vertical concentrated load F_y applied to a free end whose static scheme is shown in Fig. 4.

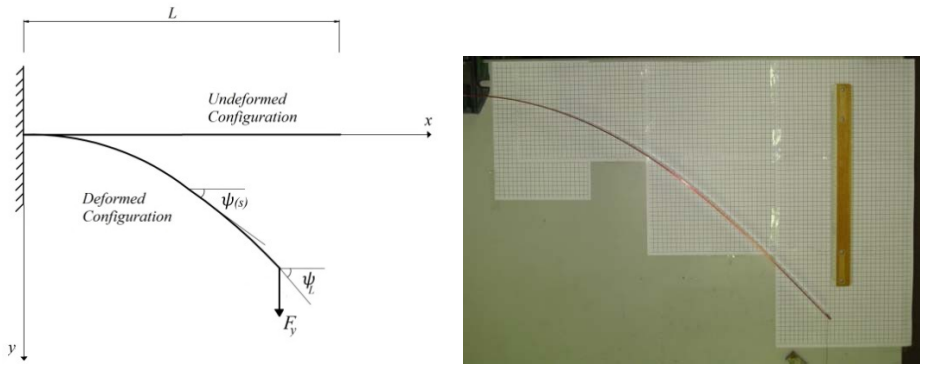

Fig. 4 Cantilever beam scheme and a picture taken during the test

This simple configuration helps to perform an experimental verification in a very simple manner, as shown in the picture. The comparison among the experimental displacements (determined by image analysis), a numerical solution obtained by Gauss integration and the analytical solution obtained through the Gauss Hypergeometric approach proposed, is given in Fig. 5. The test was conducted on an aluminum rectangular beam having Young's modulus $E = 70 \cdot 10^9\ Pa$, $920\ mm$ long, $25\ mm$ wide, $2\ mm$ thick, supporting a mass of $0.2725\ kg$ at the free end.
The comparison shows a remarkable correspondence among the three methods. The matching is comparable with the uncertainty given by experiments, mainly due to non-controllable damping effects.

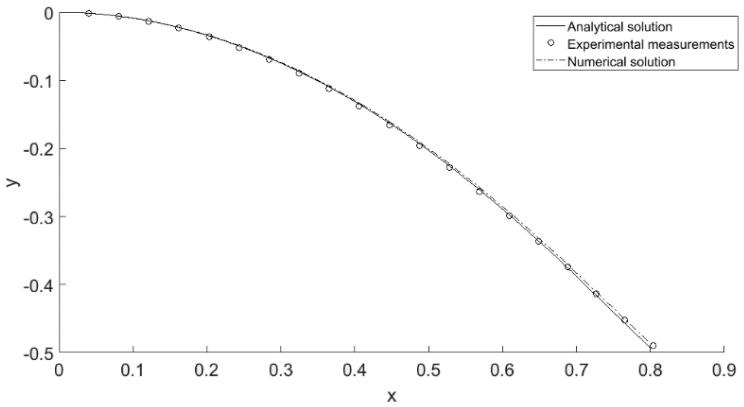

Fig.5 Comparison between the analytical solution, experimental test and numerical solution

4.2 Straight cantilever beam subjected to buckling

The analytical solution of a cantilever beam subjected to a buckling load can be obtained by imposing $F_y = 0$ in the case examined in § 3.1.
The comparison to large displacement Buckling is given in Fig.6 (a), note that the load is oriented vertically in the figure. It concerns a straight beam having Young's modulus $E = 2{,}1\ 10^{11}\ Pa$, 1000 mm long, 30 mm wide, 2 mm thick, with a buckling load $F = 1.3\ F_{cr}$ where $F_{cr} = (\pi^4/4L^2)EI = 10.36\ N$ is the Euler's critical load.

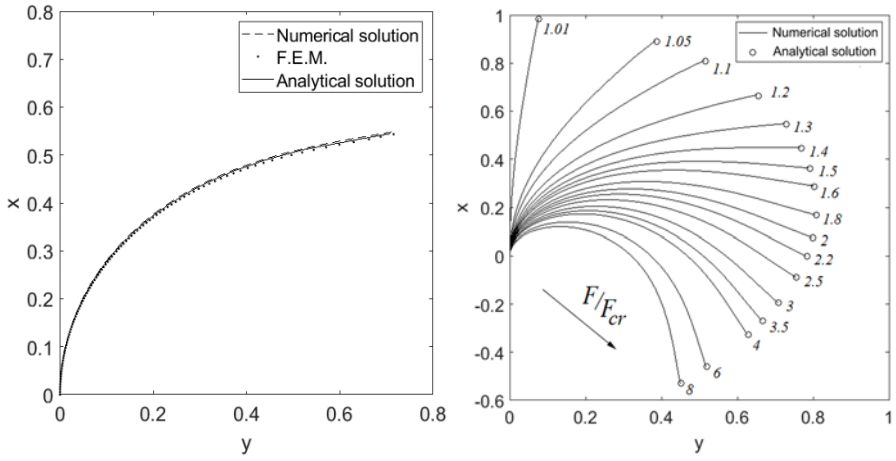

(a) (b)

Fig. 6. (a) Comparison between the analytical solution, F.E.M. solution and numerical solution of a cantilever beam subjected to a buckling load; (b) deformed configurations as a function of the ratio F/F_{cr}

In Fig.6 (b) the ratio of the applied load to the Euler critical one spans from 1 to 8, showing an increasing curvature level, as expected. The whole solution is obtained through numerical integration and is compared with the analytical solution only at the point of maximum displacement through small circles (free end). This allows to point out that the analytical solution is able to obtain the displacement of a single point, avoiding integrate throughout the whole beam.

4.3 Hinge - roller supporting a curved beam loaded in the middle

This paragraph shows an example of the application of the results obtained on an initially curved hinge-roller supported beam loaded in the middle (Fig 7).
Observe that at the middle point $\psi = 0$ and it is therefore possible to consider the double supported beam as two half-long beams locked at the middle point and loaded at the point where the support acts.
In the example in Fig.8 the beam has an initial curvature $k_0 = 1\ m^{-1}$, Young's modulus $E = 70\ 10^9$ Pa, 500 m long, 30 mm wide, 2 mm thick subject to force $F = 15\ N$.

To obtain the solution shown in Fig. 8 used the analytic solution find in paragraph 3.2 imposing $F_x = 0$.

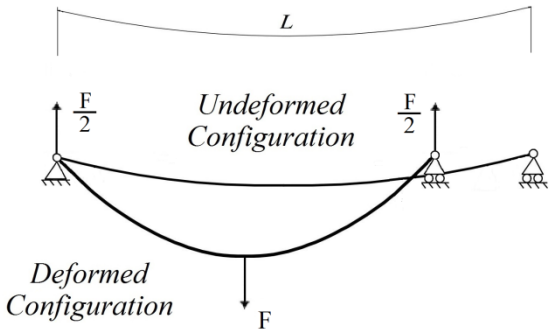

Fig. 7. Scheme of hinge-roller support initially curved beam

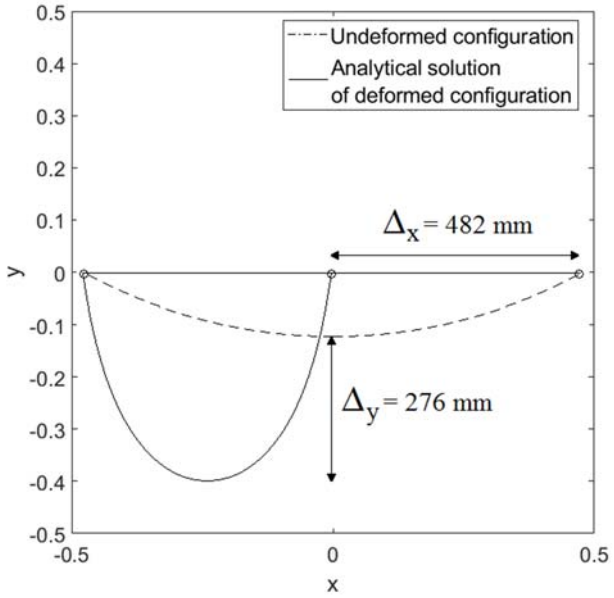

Fig. 8. Undeformed and deformed shape beam

5 Conclusion

Large deflected beams have been approached by a new technique for the solving of the differential equations. This allowed to integrate in a closed form a solution built up of a series of functions. Both curved or straight beams have been faced. The solution, similar in the analytical strategy, takes a different form when the beam is loaded

in its center line by a tension or a compression load. The convergence of the series to the correct solution (here the F.E.M. is used for comparison) has not been discussed for brevity. However, important pieces of the series can be solved once and gathered for further computations. This allows to increase considerably the speed of the procedure. One of the main advantage of the analytical solution, over direct numerical integration of the equations, is that it sounds as an input-output approach without the need to consider the variation of the physical response allover the beam.
The results obtained agree, at the limit of the numerical approximation, with F.E.M evidences, numerical integrated method and, at least for one test, with the experiment. As expected, the higher is the load, the higher is the number of elements to consider in the series. Other configurations, exploiting the same approach, will be considered in further researches.

6 Mathematical appendix

In this section, some useful notions are recalled and the fundamental mathematical steps that led to the solutions seen in section 3 are carried out.

6.1 Generalized binomial expansion

Being $x_1, x_2 \in \mathbb{R}$:

$$(x_1 + x_2)^{\alpha} = \sum_{n=0}^{\infty} \binom{\alpha}{n} {x_1}^{\alpha-n} {x_2}^{n}$$

where $|x_1| > |x_2|$, $\binom{\alpha}{n}$ is the binomial coefficient

6.2 Gaussian Hypergeometric function

The Gaussian Hypergeometric function ${}_2F_1(a, b; c; f(z))$ is a special function which belongs to the family of generalized hypergeometric functions, and is represented by this hypergeometric series:

$${}_2F_1(a, b; c; f(z)) = \sum_{k=0}^{\infty} \frac{(a)^{\bar{n}}(b)^{\bar{n}}}{(c)^{\bar{n}}} \frac{(f(z))^k}{k!}$$

Where $a \in \mathbb{R},\ n \in \mathbb{N}\ \ (a)^{\bar{n}} = a(a+1)(a+2)\ldots(a+n-1)$ is a rising factorial or called Pochhammer symbol
Useful properties of the Pochhammer coefficients are:

1) $(a)^{\bar{n}} = (-1)^n \binom{-a}{n} n!$

2) $(a)^{\bar{n}} = \frac{\Gamma(a+n)}{\Gamma(a)}$

3) $\dfrac{1}{a\,n+1} = \dfrac{\left(\frac{1}{a}\right)^{\bar{n}}}{\left(1+\frac{1}{a}\right)^{\bar{n}}}$

6.3 Special integral of eq. (11)

$a, \psi \in \mathbb{R}$, $\cos(\vartheta) - a > 0 \quad \forall\, \vartheta \in [\alpha, \psi + \alpha]$:

$$I_1(\psi) = \int_{\alpha}^{\psi+\alpha} \frac{cos(\vartheta)}{\sqrt{cos(\vartheta) - a}} d\vartheta = \int_{\alpha}^{\psi+\alpha} [cos(\vartheta) - a]^{-\frac{1}{2}}\, dsin(\vartheta) =$$

$$= \int_{\alpha}^{\psi+\alpha} \sum_{n=0}^{\infty} \binom{-\frac{1}{2}}{n} [cos(\vartheta)]^{-\frac{1}{2}\,n}\ (-a)^n\, dsin(\vartheta) =$$

The series of functions is uniformly convergent being it a series of powers with convergence radius <1 and it's possible to apply the series-integral exchange

$$I_1(\psi) = \sum_{n=0}^{\infty} (-1)^n \binom{-\frac{1}{2}}{n} (a)^n \int_{\alpha}^{\psi+\alpha} [cos(\vartheta)]^{-\frac{1}{2}-n} d\, sin(\vartheta) =$$

$$= \sum_{n=0}^{\infty} \frac{\left(\frac{1}{2}\right)^{\bar{n}}}{n!} (a)^n \int_{\alpha}^{\psi+\alpha} [1 - sin^2(\vartheta)]^{-\left(\frac{n}{2}+\frac{1}{4}\right)} d\, sin(\vartheta) =$$

$$= \sum_{n=0}^{\infty} \frac{\Gamma\left(\frac{1}{2}+n\right)}{\Gamma\left(\frac{1}{2}\right) n!} (a)^n \int_{\alpha}^{\psi+\alpha} \sum_{k=0}^{\infty} \binom{-\frac{n}{2}-\frac{1}{4}}{k} (-1)^k\, [sin^2(\vartheta)]^k\, dsin(\vartheta) =$$

$$= \sum_{n=0}^{\infty} \frac{\Gamma\left(\frac{1}{2}+n\right)}{\Gamma\left(\frac{1}{2}\right) n!} (a)^n \left[\sum_{k=0}^{\infty} \frac{\left(\frac{n}{2}+\frac{1}{4}\right)^{\bar{k}}}{k!} \int_{\alpha}^{\psi+\alpha} [sin^2(\vartheta)]^k\, dsin(\vartheta) \right] =$$

$$= \sum_{n=0}^{\infty} \frac{\Gamma\left(\frac{1}{2}+n\right)}{\Gamma\left(\frac{1}{2}\right) n!} (a)^n \left[\sum_{k=0}^{\infty} \frac{\left(\frac{2n+1}{4}\right)^{\bar{k}} \left(\frac{1}{2}\right)^{\bar{k}}}{\left(\frac{3}{2}\right)^{\bar{k}}} \frac{[sin(\vartheta)]^{2k+1}\Big|_{\alpha}^{\psi+\alpha}}{k!} \right] =$$

$$= \sum_{n=0}^{\infty} \frac{\Gamma\left(\frac{1}{2}+n\right)}{\Gamma\left(\frac{1}{2}\right) n!} (a)^n \left[{}_2F_1\left(\frac{1}{2}, \frac{2n+1}{4}; \frac{3}{2}; \sin^2(\psi+\alpha)\right) \sin(\psi+\alpha) + \right.$$

$$\left. - {}_2F_1\left(\frac{1}{2}, \frac{2n+1}{4}; \frac{3}{2}; \sin^2(\alpha)\right) \sin(\alpha) \right]$$

6.4 Special integral of eq. (13)

$a,\ \psi_L\ \in \mathbb{R}\ ,\ cos(\vartheta) - a > 0\ \ \forall\, \vartheta \in [\alpha, \psi_L + \alpha]$:

$$I_2 = \int_{\alpha}^{\psi_L+\alpha} \frac{d\vartheta}{\sqrt{cos(\vartheta) - a}} = \int_{\alpha}^{\psi_L+\alpha} [cos(\vartheta) - a]^{-\frac{1}{2}}\, d\vartheta =$$

$$= \int_{\alpha}^{\psi_L+\alpha} \sum_{n=0}^{\infty} \binom{-\frac{1}{2}}{n} (-a)^{\,n}\, [cos(\vartheta)]^{-\frac{1}{2}-n} d\vartheta =$$

By applying the series-integral exchange:

$$I_2 = \sum_{n=0}^{\infty} \frac{\left(\frac{1}{2}\right)^{\bar{n}}}{n!} (a)^n \int_{\alpha}^{\psi_L+\alpha} [cos(\vartheta)]^{-\frac{3}{2}-n}\, dsin(\vartheta) =$$

$$= \sum_{n=0}^{\infty} \frac{\left(\frac{1}{2}\right)^{\bar{n}}}{n!} (a)^n \int_{\alpha}^{\psi_L+\alpha} [1 - sin^2(\vartheta)]^{-\left(\frac{3}{4}+n\right)}\, dsin(\vartheta) =$$

$$= \sum_{n=0}^{\infty} \frac{\Gamma\left(\frac{1}{2}+n\right)}{\Gamma\left(\frac{1}{2}\right)\, n!} (a)^n \int_{\alpha}^{\psi_L+\alpha} \sum_{k=0}^{\infty} \binom{-\frac{3}{4}-\frac{n}{2}}{k} [-sin^2(\vartheta)]^k\, dsin(\vartheta) =$$

$$= \sum_{n=0}^{\infty} \frac{\Gamma\left(\frac{1}{2}+n\right)}{\Gamma\left(\frac{1}{2}\right)\, n!} (a)^n \left[\sum_{k=0}^{\infty} \frac{\left(\frac{2n+3}{4}\right)^{\bar{k}}}{k!} \int_{\alpha}^{\psi_L+\alpha} [sin(\vartheta)]^{2k}\, dsin(\vartheta) \right] =$$

$$= \sum_{n=0}^{\infty} \frac{\Gamma\left(\frac{1}{2}+n\right)}{\Gamma\left(\frac{1}{2}\right)\, n!} (a)^n \left[\sum_{k=0}^{\infty} \frac{\left(\frac{2n+3}{4}\right)^{\bar{k}} \left(\frac{1}{2}\right)^{\bar{n}}}{\left(\frac{3}{2}\right)^{\bar{n}}} \frac{[sin(\psi_L + \alpha)]^{2k+1} - [sin(\alpha)]^{2k+1}}{k!} \right] =$$

$$= \sum_{n=0}^{\infty} \frac{\Gamma\left(\frac{1}{2}+n\right)}{\Gamma\left(\frac{1}{2}\right)\, n!} (a)^n \left[{}_2F_1\left(\frac{1}{2}, \frac{2n+3}{4}; \frac{3}{2}; \sin^2(\psi_L + \alpha)\right) \sin(\psi_L + \alpha) + \right.$$

$$\left. - {}_2F_1\left(\frac{1}{2}, \frac{2n+3}{4}; \frac{3}{2}; \sin^2(\alpha)\right) \sin(\alpha) \right]$$

6.5 Special integral of eq. (14)

$a,\ \psi\ \in \mathbb{R}\ ,\ a - \sin(\vartheta) > 0\ \ \forall\, \vartheta \in [\alpha, \psi + \alpha]$:

$$I_3(\psi) = \int_{\alpha}^{\psi+\alpha} \frac{sin(\vartheta)}{\sqrt{a - sin(\vartheta)}} d\vartheta = -\int_{\alpha}^{\psi+\alpha} [a - \sin(\vartheta)]^{-\frac{1}{2}}\, dcos(\vartheta)\ =$$

$$= -\int_{\alpha}^{\psi+\alpha} \sum_{n=0}^{\infty} \binom{-\frac{1}{2}}{n} (a)^{-\frac{1}{2}-n} \, [-\sin(\vartheta)]^n \, dcos(\vartheta) =$$

By applying the series-integral exchange:

$$I_3(\psi) = \sum_{n=0}^{\infty} (-1)^n \binom{-\frac{1}{2}}{n} (a)^{-\frac{1}{2}-n} \int_{\psi+\alpha}^{\alpha} [sin(\vartheta)\,]^n \, dcos(\vartheta) =$$

$$= \sum_{n=0}^{\infty} \frac{\left(\frac{1}{2}\right)^{\bar{n}}}{n!} (a)^{-\frac{1}{2}-n} \int_{\psi+\alpha}^{\alpha} [1 - cos^2(\vartheta)]^{\frac{n}{2}} \, dcos(\vartheta) =$$

$$= \sum_{n=0}^{\infty} \frac{\Gamma\left(\frac{1}{2}+n\right)}{\Gamma\left(\frac{1}{2}\right) n!} (a)^{-\frac{1}{2}-n} \int_{\psi+\alpha}^{\alpha} \sum_{k=0}^{\infty} \binom{\frac{n}{2}}{k} (-1)^k [cos(\vartheta)]^{2k} \, dcos(\vartheta) =$$

$$= \sum_{n=0}^{\infty} \frac{\Gamma\left(\frac{1}{2}+n\right)}{\Gamma\left(\frac{1}{2}\right) n!} (a)^{-\frac{1}{2}-n} \left[\sum_{k=0}^{\infty} \frac{\left(-\frac{n}{2}\right)^{\bar{k}}}{k!} \int_{\psi+\alpha}^{\alpha} [cos(\vartheta)]^{2k} \, dcos(\vartheta) \right] =$$

$$= \sum_{n=0}^{\infty} \frac{\Gamma\left(\frac{1}{2}+n\right)}{\Gamma\left(\frac{1}{2}\right) n!} (a)^{-\frac{1}{2}-n} \left[\sum_{k=0}^{\infty} \frac{\left(-\frac{n}{2}\right)^{\bar{k}} \left(\frac{1}{2}\right)^{\bar{k}}}{\left(\frac{3}{2}\right)^{\bar{k}}} \, \frac{[cos(\vartheta)]^{2k+1}\Big|_{\psi+\alpha}^{\alpha}}{k!} \right] =$$

$$= \sum_{n=0}^{\infty} \frac{\Gamma\left(\frac{1}{2}+n\right)}{\Gamma\left(\frac{1}{2}\right) n!} (a)^{-\frac{1}{2}-n} \Big[{}_2F_1\left(\frac{1}{2}, -\frac{n}{2}; \frac{3}{2}; cos^2(\alpha)\right) cos(\alpha) +$$

$$- {}_2F_1\left(\frac{1}{2}, -\frac{n}{2}; \frac{3}{2}; cos^2(\psi+\alpha)\right) cos(\psi+\alpha) \Big]$$

6.6 Special integral of eq. (15)

$a, \psi_L \in \mathbb{R}$, $cos(\vartheta) - a > 0 \;\; \forall \, \vartheta \in [\alpha, \psi_L + \alpha]$:

$$I_4 = \int_{\alpha}^{\psi_L+\alpha} \frac{d\vartheta}{\sqrt{a - sin(\vartheta)}} = \int_{\alpha}^{\psi_L+\alpha} [a - sin(\vartheta)]^{-\frac{1}{2}} \, d\vartheta =$$

$$= \int_{\alpha}^{\psi_L+\alpha} \sum_{n=0}^{\infty} \binom{-\frac{1}{2}}{n} (a)^{-\frac{1}{2}-n} \, [-sin(\vartheta)]^{\,n} \, d\vartheta =$$

By applying the series-integral exchange:

$$I_4 = -\sum_{n=0}^{\infty} \frac{\left(\frac{1}{2}\right)^{\bar{n}}}{n!} (a)^{-\frac{1}{2}-n} \int_{\alpha}^{\psi_L+\alpha} [sin(\vartheta)]^{n-1}\, dcos(\vartheta) =$$

$$= \sum_{n=0}^{\infty} \frac{\left(\frac{1}{2}\right)^{\bar{n}}}{n!} (a)^{-\frac{1}{2}-n} \int_{\psi_L+\alpha}^{\alpha} [1-cos^2(\vartheta)]^{\frac{n-1}{2}}\, dcos(\vartheta) =$$

$$= \sum_{n=0}^{\infty} \frac{\Gamma\left(\frac{1}{2}+n\right)}{\Gamma\left(\frac{1}{2}\right)\, n!} (a)^{-\frac{1}{2}-n} \int_{\psi_L+\alpha}^{\alpha} \sum_{k=0}^{\infty} \binom{n-1}{k} [-cos^2(\vartheta)]^k\, dcos(\vartheta) =$$

$$= \sum_{n=0}^{\infty} \frac{\Gamma\left(\frac{1}{2}+n\right)}{\Gamma\left(\frac{1}{2}\right)\, n!} (a)^{-\frac{1}{2}-n} \left[\sum_{k=0}^{\infty} \frac{\left(\frac{1-n}{2}\right)^{\bar{k}}}{k!} \int_{\psi_L+\alpha}^{\alpha} [cos(\vartheta)]^{2k}\, dcos(\vartheta) \right] =$$

$$= \sum_{n=0}^{\infty} \frac{\Gamma\left(\frac{1}{2}+n\right)}{\Gamma\left(\frac{1}{2}\right)\, n!} (a)^{-\frac{1}{2}-n} \left[\sum_{k=0}^{\infty} \frac{\left(\frac{1-n}{2}\right)^{\bar{k}} \left(\frac{1}{2}\right)^{\bar{n}}}{\left(\frac{3}{2}\right)^{\bar{n}}} \frac{[cos(\alpha)]^{2k+1} - [cos(\psi_L+\alpha)]^{2k+1}}{k!} \right] =$$

$$= \sum_{n=0}^{\infty} \frac{\Gamma\left(\frac{1}{2}+n\right)}{\Gamma\left(\frac{1}{2}\right)\, n!} (a)^{-\frac{1}{2}-n} \left[{}_2F_1\left(\frac{1}{2}, \frac{1-n}{4}; \frac{3}{2}; \cos^2(\alpha)\right) \cos(\alpha) + \right.$$

$$\left. - {}_2F_1\left(\frac{1}{2}, \frac{1-n}{4}; \frac{3}{2}; \cos^2(\psi_L+\alpha)\right) \cos(\psi_L+\alpha) \right]$$

References

1. D.H. Hodges, R.A. Orniston , Stability of elastic bending and torsion of uniform cantilever rotor blades in hover with variable structural coupling, National Aeronautics and space administration (NASA), Washington D.C. , 1976.
2. C.Truesdell , Leonhard Euler , The rational mechanics of flexible or elastic bodies 1638-1788, Birkhäuser Basel, 1960.
3. H. J. Barten , On the deflection of a Cantilever Beam, Quarterly of Applied Mathematics, 2, 168-171 , 1944.
4. K.E. Bisshop, D.C. Drucker, Large deflection of cantilever beams , Quarterly of Applied Mathematics 3 ,272–275 , 1945.
5. A.Banerjee, B.Bhattacharya, A.K. Mallik, Large deflection of a cantilever beams with geometric non-linearity: Analytical and numerical approaches, International Journal of Non-Linear Mechanics, vol.43 366-376, 2008.
6. Hafez Tari, On a parametric large deflection study of Euler-Bernoulli cantilever beams subjected to a combined tip point loading , International Journal of Non-Linear Mechanics, vol.49 90-99, 2013.
7. B.S. Shvartsman, Analysis of large deflections of a curved cantilever subjected to a tip-concentrated follower force, International Journal of Non-Linear Mechanics, vol.50 75-80, 2013.

8. A. K. Nallathambi, C. Lakshmana Rao, S.M. Srinivasan, Large deflection of a constant curvature cantilever beam under follower load , International Journal of Mechanical Sciences , vol.52 440-445, 2010.
9. Reissner, On one dimensional finite strain beam theory: the plane problem , Journal of Applied Mathematics and Physics (ZAMP), vol.23 , 1972.
10. B.C.Carlson , Some series and bounds for incomplete elliptic integrals, Journal of Mathematics and Physics, vol. 40125-134, 1961.
11. L. Landau , Theory of elasticity , translated from Russian by J. B. Sykes and W. H. Elsevier Reid , Pergamon Press, London, 1959.
12. R. Frish-Fay, Flexible bars, Butterworths , London, 1962.
13. O.Belluzzi, Scienza delle costruzioni vol.4, Zanichelli,Bologna,1998.
14. S. Timoshenko, J.M. Gere, Theory of elastic stability, McGraw –Hill, 1963.
15. Hafez T. , On the parametric large deflection study of Euler–Bernoulli cantilever beams subjected to combined tip point loading , International Journal of Non-Linear Mechanics vol.49, 90–99, 2013.
16. Vivek A. Jairazbhoy; Pavel Petukhov; Jianmin Qu, M.Asce, Large deflection of thin plates in convex or concave cylindrical Bending , Journal of Engineering Mechanics ,vol.138, 230-234, 2011.
17. F.De Bona, S.Zelenika, A generalized elastica-type approach to the analysis of large displacements of spring-strips ,Journal of Mechanical Engineering Science,vol.211, 509-517, 1997.
18. John C. Visner,, Analytical and experimental analysis of the large deflection of a cantilever beam subjected to a constant, concentrated force, with constant angle, applied at the free end ,A thesis presented to the graduate faculty of the university of akron,2007.
19. B.S. Shvartsman, Analysis of large deflections of a curved cantilever subjected to a tip-concentrated follower force, International Journal of Non-Linear Mechanics vol.50 ,75–80, 2013.
20. Howell P. D. , Kozyreff G. , Ockendon R. , Applied solid mechanics , Cambridge university press, New York, 2009.
21. Magnus.W, Oberhettinger F. , Tricomi F. G. , Higher trascendental functions vol.1 , McGraw-Hill , New York,1953.